Transcript profiling of CD16-positive monocytes reveals a unique molecular fingerprint

Marion Frankenberger¹, Thomas P.J. Hofer¹, Ayman Marei², Farshid Dayyani², Stefan Schewe³, Christine Strasser³, Asaad Aldraihim², Franz Stanzel¹, Roland Lang⁴, Reinhard Hoffmann⁴, Olivia Prazeres da Costa⁴, Thorsten Buch⁴ and Loems Ziegler-Heitbrock^{1,2}

- ¹ Comprehensive Pneumology Center Helmholtz Zentrum München, Ludwig-Maximilians University and Asklepios Fachklinik Gauting, Munich, Germany
- ² Department of Infection Immunity and Inflammation, University of Leicester, Leicester, UK
- ³ Policlinic of Internal Medicine Department of Rheumatology, Ludwig-Maximilians-University, Munich, Germany
- ⁴ Institute for Medical Microbiology Immunology and Hygiene, Technische Universität München, Munich, Germany

CD16-positive (CD14++CD16+ and CD14+CD16++) monocytes have unique features with respect to phenotype and function. We have used transcriptional profiling for comparison of CD16-positive monocytes and classical monocytes. We show herein that 187 genes are greater than fivefold differentially expressed, including 90 genes relevant to immune response and inflammation. Hierarchical clustering of data for monocyte subsets and CD1c+ myeloid blood dendritic cells (DCs) demonstrate that CD16-positive cells are more closely related to classical monocytes than to DCs. Reverse transcriptase polymerase chain reaction for ten genes with the strongest differential expression confirmed the pattern including a lower messenger RNA level for CD14, CD163, and versican in CD16positive monocytes. The pattern was similar for CD16-positive monocytes at rest and after exercise mobilization from the marginal pool. By contrast, alveolar macrophages, small sputum macrophages, breast milk macrophages, and synovial macrophages all showed a different pattern. When monocyte-derived macrophages (MDMs) were generated from CD16-positive monocytes by culture with macrophage colony-stimulating factor in vitro, then the MDMs maintained properties of their progeny with lower expression of CD14, CD163, and versican compared with CD14++CD16- MDMs. Furthermore, CD16-positive MDMs showed a higher phagocytosis for opsonized Escherichia coli. The data demonstrate that CD16-positive monocytes form a distinct type of cell, which gives rise to a distinct macrophage phenotype.

Keywords: CD16 · Dendritic cells · Gene expression · Macrophages · Monocytes



Supporting Information available online

Introduction

In human blood two populations of monocytes can be identified, that is, the classical CD14⁺⁺CD16⁻ monocytes, which are defined based on high expression of CD14, the nonclassical CD14⁺CD16⁺⁺ monocytes, which coexpress CD16 together with

Correspondence: Prof. Loems Ziegler-Heitbrock e-mail: ziegler-heitbrock@helmholtz-muenchen.de

low levels of CD14 and the intermediate CD14++CD16+ monocytes (for nomenclature see Ziegler-Heitbrock et al. [1]). The latter two populations can be collectively addressed as CD16-positive monocytes. The CD16-positive monocytes when compared with the classical monocytes have been shown to express higher levels of LPS-induced TNF production, while IL-10 expression is low to absent. Also, the former cells have been reported to increase in various inflammatory conditions and to decrease with glucocorticoid therapy [2-6] pointing toward an important role of these cells in disease. A gradual transition from classical CD14⁺⁺CD16⁻ monocytes to nonclassical CD14+CD16++ monocytes has been observed during macrophage colony-stimulating factor (M-CSF) therapy [7] and a detailed analysis of gene expression in the three subtypes of monocytes has shown a gradual increase or decrease in expression of markers from classical, to intermediates and nonclassical monocytes [8]. These findings are in line with the concept that there is a developmental relationship from the less mature classical to the more mature nonclassical monocytes.

Monocytes circulate in the blood for 1–3 days and then migrate into tissue where they develop into macrophages or dendritic cells (DCs). Tissue macrophages are known to be heterogeneous with respect to phenotype and function and this is dependent on the type of tissue and on pathophysiological processes such as inflammation or tumor growth. With heterogeneity at the level of the blood monocyte, the question is whether a given blood monocyte subset is committed to becoming a unique type of macrophage in tissue.

In order to address this question, we have analyzed CD16-positive monocytes, CD16-negative classical monocytes and the macrophages generated from these cells in vitro, and have compared the gene expression of these cells, the CD1c⁺ blood DCs and a set of different types of tissue macrophages.

Our data show that CD16-positive monocytes cluster with classical monocytes and not with CD1c⁺ DCs and that they develop into macrophages that are clearly distinct from macrophages derived from classical monocytes and from different types of tissue macrophages.

Results

Differential gene expression between CD14⁺⁺CD16⁻ monocytes and CD16-positive monocytes

To study gene expression, we isolated the two types of monocytes by magnetic-activated cell sorting (MACS) technology in the cold and determined their purity by flow cytometry. As shown in Fig. 1A and B both classical and CD16-positive monocytes, consisting of nonclassical and a small population of intermediate monocytes, had purities in excess of 95%. Cells from three donors were used to purify the messenger RNA (mRNA), which was labeled and hybridized to the Affymetrix U133 plus2 chip (Freiburg, Germany). The gene expression data have been used in Ingersoll et al. [9] and are available under accession number GSE18565 in the GEO data bank.

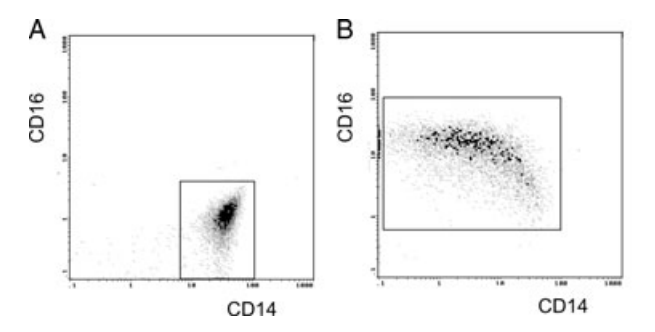


Figure 1. Purity of isolated blood monocyte subsets. Mononuclear cells were isolated from peripheral blood by density gradient separation and monocytes were purified by positive selection using magnetic-activated cell sorting (MACS) technology. Shown are dot plots of the FACS analysis of (A) classical monocytes, purity 99% and (B) nonclassical monocytes, purity 97%. Data are representative of three experiments.

Using these data sets, we took the average readings from the three donors and selected transcripts for which the difference between the two types of monocytes was ≥ 100 units and for which the ratio in expression was ≥ 5 . In addition, differences had to be statistically significant as defined by a Limma F-test p-value <0.01. These criteria were fulfilled by 187 genes. These data were subjected to hierarchical clustering and are presented as a heat map (Fig. 2). As can be seen, there is some variation between individuals in that there are a few islands of genes with low expression (green) within the high expression fields (red). Still, it is clear that in average there is differentially high and low expression in all three individuals for all the genes shown. These 187 genes listed in Table 1 were assigned to biological processes using gene ontology annotation [10].

The differentially expressed genes mainly are associated with processes of immune response and inflammation. Also, there are differentially expressed genes involved in processes of signal transduction, adhesion, chemotaxis, and cell death. The latter types of genes affect the action and fate of monocytes. Since monocytes are important to immunoregulation, the differential expression of these genes will impact on the immune response and inflammation, as well. In addition there are differential signatures for transmembrane transport, electron transport, RNA degradation, lipid metabolism, and angiogenesis. Finally there are genes without annotation, which show a strongly increased transcript level in the CD16-positive monocytes and this includes a more than 70-fold higher expression for LOC200772 and a more than 60-fold higher expression for SH2D1B.

We then selected five immunologically relevant genes for RT-PCR confirmation and analysis at the protein level. As shown in Supporting Information Fig. 1A, the mRNA for CD89 (Fc α RI) and for CD163 (haemoglobin scavenger receptor) show a very low level of expression in the CD16-positive monocytes. Analysis of the protein expression for these molecules by FACS demonstrates a low-level expression for these cell-surface receptors, as well (Supporting Information Fig. 1B and C). RT-PCR analysis for the IL-21 receptor, CD79b (immunoglobulin-associated beta chain), and CD122 (IL-2 receptor beta chain) demonstrates a much higher

Eur. J. Immunol. 2012. 42: 957–974 Innate immunity

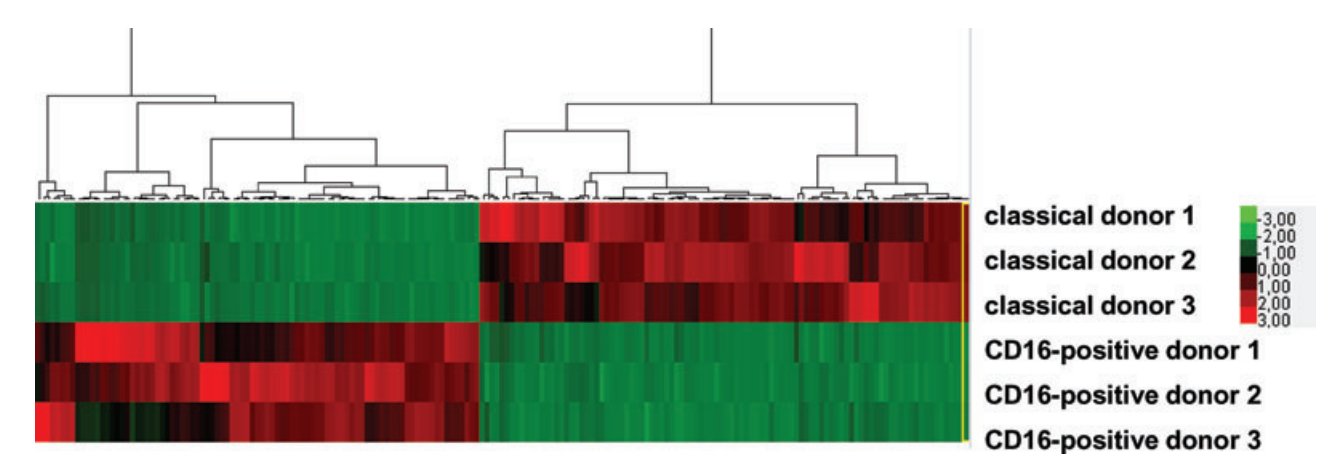


Figure 2. Heat map showing the hierarchical clustering of the two monocyte subsets. Monocyte subsets were isolated from three donors and messenger RNA (mRNA) was isolated, labeled, and hybridized to Affymetrix U133 plus2.arrays. Data are from Affymetrix gene expression arrays. Genes were selected based on differential expression of at least 100 units with a ratio of at least fivefold. Shown are the results for the three individuals studied.

expression of the transcripts in the CD16-positive monocytes as compared with the classical monocytes (Supporting Information Fig. 1A). Again, analysis of protein expression shows a similar pattern (Supporting Information Fig. 1D–F) with much higher levels of expression in the CD16-positive monocytes. All differences were statistically significant (see Supporting Information Table 1). Taken together, the RT-PCR analysis confirms the findings in the array analysis and the protein expression also shows a congruent pattern.

Comparison of monocyte subpopulations with $CD1c^+$ DCs

Since the CD16-positive monocytes compared with the classical monocytes have a higher propensity to develop into DCs [11], we then tested the relationship of these monocytes to the CD1c⁺ blood DCs by comparing their transcriptome. The CD1c⁺ blood DCs were also isolated by MACS technology and FACS analysis was performed (Fig. 3).

While the level of expression of CD1c is low and overlaps with the isotype control staining, more than 96% of the cells are CD1c $^+$. This is since they are part of the monomodal distribution that is shifted to the right relative to the isotype control, that is, they are to the right of the dotted line in Fig. 3. From such purified DCs of three donors, mRNA was isolated, labeled, and hybridized to the Affymetrix U133 plus2 chip.

After RMA normalization, the overall expression levels from cell (CEL) files were subjected to hierarchical clustering of the samples. The degree of similarity is represented by the tree and the distance level by the height of the tree. As shown in Fig. 4, the respective cell types of the three donors cluster together. Further, it is apparent that the two monocyte subsets are more closely related to each other and are both distinct from the CD1c $^+$ DCs. Hence, these data show that the CD16-positive cells are closely related to

the classical monocytes and are to be classified as monocytes and not DCs

Gene expression in CD16-positive monocytes at rest and after exercise

We then focused on the monocyte subsets and selected from the 187 genes a set of ten genes with a high level of expression with >1000 arbitrary units in either the classical or the CD16-positive monocytes. Among these, the genes with lower expression in CD16-positive monocytes as compared with the classical monocytes were CD163, versican, RNase k6 (ribonuclease family k6), and MGST1. On the other hand genes with clearly higher expression in the CD16-positive monocytes were cutlike1, rhoC, LOC200772, and Kip2 (Table 1). In addition, we looked at the CD16 gene known to show higher mRNA expression and the CD14 gene known to be lower at the mRNA level in the CD16-positive monocytes [12].

The differential expression of all these genes was analyzed by RT-PCR in a new set of highly purified monocyte subsets taken from three independent donors at rest and after exercise. The RT-PCR data of the cells at rest confirmed the differential expression seen in the array analysis. The average expression is more than 100-fold higher in the CD16-positive monocytes for CD16, Kip2, and LOC200772 and it is more than tenfold lower for CD14, CD163, and versican (Fig. 5A). When donors are subjected to short periods of exercise there is a strong increase in CD16-positive monocytes. These cells likely derive from the marginal pool [13], that is, under resting conditions, they reside in the slow flowing lining fluid of the vasculature. We asked whether the cells in the marginal pool form a distinct population of cells or whether the CD16-positive monocytes from the central pool and the marginal pool are identical. Mobilization by exercise on a home trainer bike in three individuals led to a 4.2-fold increase ± 1.0 in the number of CD16-positive monocytes. This implies that about 75% of cells

 Table 1. Genes with more than fivefold differential expression in monocyte subpopulations

960

Probe set ID	Gene title	Classical	CD16- pos	Ratio	Gene symbol	Gene ontology biological process
205297_s_at	CD79b molecule, immunoglobulin-associated	70	709	10,11	CD79B	Immune response
204006_s_at	beta CD16a	74	5961	90 97	FCGR3A	Immuno rosponso
204006_S_at 210140_at	Cystatin F (leukocystatin)	74 44	268	80,87 6,06	CST7	Immune response Immune response
210140_at 211796_s_at	T cell receptor beta variable 19 /	35	189	5,40	TRBV19	Immune response
227354_at	Phosphoprotein associated with glycosphingolipid microdomains 1	195	1091	5,58	PAG1	Immune response
218638_s_at	Spondin 2, extracellular matrix protein	78	415	5,29	SPON2	Immune response
202953_at	Complement component 1, q subcomponent, B chain	41	439	10,57	C1QB	Immune response
218232_at	Complement component 1, q subcomponent, A chain	108	1166	10,78	C1QA	Immune response
214450_at	Cathepsin W	64	379	5,97	CTSW	Immune response
202087_s_at	Cathepsin L1	260	1472	5,67	CTSL1	Immune response
216705_s_at	Adenosine deaminase	112	1511	13,44	ADA	Immune response
203921 ₋ at	Carbohydrate (N-acetylglucosamine-6-0) sulfotransferase 2	221	2132	9,64	CHST2	Inflammatory response
37145_at	Granulysin	55	685	12,44	GNLY	Defense response to bacterium
214199_at	Surfactant, pulmonary-associated protein D	39	249	6,31	SFTPD	Cytokine production
221658_s_at	Interleukin 21 receptor	22	416	19,33	IL-21R	Natural killer cell activation
205291_at	Interleukin 2 receptor, beta	78	638	8,13	IL-2RB	Cytokine and chemokine mediated signaling pathway
205419 ₋ at	Epstein–Barr virus induced gene 2 (lymphocyte-specific GPCR)	1251	97	0,08	EBI2	Immune response
207674_at	Fc fragment of IgA, receptor for	700	131	0,19	FCAR	Immune response
219890_at	C-type lectin domain family 5, member A	159	12	0,07	CLEC5A	Immune response
1552773 ₋ at	C-type lectin domain family 4, member D	567	26	0,05	CLEC4D	Immune response
222934_s_at	C-type lectin domain family 4, member E	1456	127	0,09	CLEC4E	Immune response
241819_at	Tumor necrosis factor (ligand) superfamily, member 8	266	37	0,14	TNFSF8	Immune response
211734_s_at	High-affinity IgE, receptor alpha	605	25	0,04	FCER1A	Immune response
209765_at	ADAM metallopeptidase domain 19	261	30	0,11	ADAM19	Immune response
201743_at	CD14 molecule	7013	709	0,10	CD14	Inflammatory response
228176_at	Endothelial differentiation, sphingolipid GPCR 3	819	35	0,04	EDG3	Inflammatory response
204150_at	Stabilin 1	968	130	0,13	STAB1	Inflammatory response
205863 ₋ at	S100 calcium binding protein A12	5965	295	0,05	S100A12	Inflammatory response
206214_at	Phospholipase A2, group VII	679	42	0,06	PLA2G7	Inflammatory response
208470_s_at	Haptoglobin-related protein	288	37	0,13	HPR	Defense response

Table 1. (Continued)

			CD16-		Gene	Gene ontology
Probe set ID	Gene title	Classical	pos	Ratio	symbol	biological process
203645_s_at	CD163 molecule	2503	83	0,03	CD163	Acute-phase response
06361_at	G protein coupled receptor 44	55	650	11,77	GPR44	Chemotaxis
03036_s_at	Metastasis suppressor 1	116	617	5,33	MTSS1	Cell motility
13488_at	Sushi, nidogen and EGF-like	30	176	5,95	SNED1	Cell adhesion
.13100_at	domains 1	30	170	3,33	SIVEDI	den danesion
22838_at	SLAM family member 7	80	553	6,94	SLAMF7	Cell adhesion
.552806_a_at	Sialic acid binding Ig-like lectin 10	175	1213	6,92	SIGLEC10	Cell adhesion
212070_at	G protein coupled receptor 56	25	169	6,75	GPR56	Cell adhesion
ŀ7069_at	Proline rich 5 (renal)	48	263	5,43	PRR5	Cell migration
15785_s_at	Cytoplasmic FMR1 interacting protein 2	302	1527	5,06	CYFIP2	Cell adhesion
06978_at	CCR2 (CD192 antigen)	2570	55	0,02	CCR2	Chemotaxis
201110_s_at	Thrombospondin 1	938	21	0,02	THBS1	Cell adhesion
04619_s_at	Versican	3670	340	0,09	VCAN	Cell adhesion
26817 ₋ at	Desmocollin 2	251	37	0,15	DSC2	Cell adhesion
04714_s_at	Coagulation factor V	507	27	0,05	F5	Cell adhesion
01029_s_at	CD99 molecule	2621	506	0,19	CD99	Cell adhesion
10164_at	Granzyme B (granzyme 2)	30	408	13,48	GZMB	Apoptosis
05488_at	Granzyme A (granzyme 1)	12	225	18,64	GZMA	Apoptosis
07500 ₋ at	Caspase 5, apoptosis-related cysteine peptidase	62	400	6,48	CASP5	Apoptosis
14617_at	Perforin 1 (pore forming protein)	31	643	20,47	PRF1	Apoptosis
04614_at	Serpin peptidase inhibitor, clade B, member 2	298	10	0,04	SERPINB2	Apoptosis
201631_s_at	Immediate early response 3	2070	289	0,14	IER3	Apoptosis
04860_s_at	NLR family, apoptosis inhibitory protein	311	54	0,17	NAIP	Apoptosis
30359_at	Kinase noncatalytic C-lobe domain (KIND) containing 1	35	274	7,91	KNDC1	Signal transduction
35816_s_at	Ral-GDS related protein Rgr	33	168	5,07	Rgr	Signal transduction
01601_x_at	Interferon induced transmembrane protein 1 (9–27)	460	4361	9,49	IFITM1	Signal transduction
14470_at	Killer cell lectin-like receptor subfamily B, member 1	29	430	14,78	KLRB1	Signal transduction
02609_at	Epidermal growth factor receptor pathway substrate 8	76	723	9,48	EPS8	Signal transduction
222942_s_at	T-cell lymphoma invasion and metastasis 2	27	305	11,22	TIAM2	Signal transduction
30464_at	Endothelial differentiation, sphingolipid GPCR 8	31	158	5,11	EDG8	Signal transduction
23344_s_at	Membrane-spanning 4-domains, subfamily A, member 7	1193	6285	5,27	MS4A7	Signal transduction
19607_s_at	Membrane-spanning 4-domains, subfamily A, member 4	296	1909	6,46	MS4A4A	Signal transduction
226837_at	sprouty-related, EVH1 domain containing 1	75	386	5,17	SPRED1	Signal transduction
227210_at	cDNA FLJ32568 fis	136	957	7,04	_	Regulation of transcription

Table 1. (Continued)

Probe set ID	Gene title	Classical	CD16- pos	Ratio	Gene symbol	Gene ontology biological process
226184_at	Formin-like 2	52	945	18,34	FMNL2	Regulation of transcription
227347_x_at	Hairy and enhancer of split 4	40	694	17,40	HES4	Regulation of transcription
224833_at	v-ets erythroblastosis virus E26 oncogene homolog 1	36	577	16,04	ETS1	Regulation of transcription
204760_s_at	Thyroid hormone receptor, alpha	57	390	6,88	NR1D1	Regulation of transcription
216511_s_at	Transcription factor 7 like 2 (T cell specific, HMG-box)	216	2429	11,24	TCF7L2	Regulation of transcription
202367_at	Cut-like homeobox 1	425	3964	9,33	CUX1	Regulation of transcription
211597_s_at	HOP homeobox	18	336	18,29	HOPX	Regulation of transcription
203394_s_at	Hairy and enhancer of split 1,	400	2034	5,09	HES1	Regulation of transcription
213182_x_at	Cyclin-dependent kinase inhibitor 1C (p57, Kip2)	99	3838	38,77	CDKN1C	Regulation of transcription
200885_at	Ras homolog gene family, member C	317	3092	9,75	RHOC	Regulation of NF-kappaB cascade
230550_at	Membrane-spanning 4-domains, subfamily A, member 6A	1615	201	0,12	MS4A6A	Signal transduction
210220_at	Frizzled homolog 2	293	51	0,17	FZD2	Signal transduction
205698_s_at	Mitogen-activated protein kinase	380	51	0,13	MAP2K6	Signal transduction
202252_at	RAB13, member Ras oncogene family	291	42	0,14	RAB13	Regulation of transcription
205249_at	Early growth response 2	769	151	0,20	EGR2	Regulation of transcription
220001_at	Peptidyl arginine deiminase, type IV	988	91	0,09	PADI4	Regulation of transcription
229228_at	cAMP responsive element binding protein 5	608	95	0,16	CREB5	Regulation of transcription
214438_at	H2.0-like homeobox	435	62	0,14	HLX	Regulation of transcription
227080_at	Zinc finger protein 697	228	30	0,13	ZNF697	Regulation of transcription
218149_s_at	Zinc finger protein 395	575	65	0,11	ZNF395	Regulation of transcription
204099_at	SWI/SNF related, subfamily d, member 3	804	112	0,14	SMARCD3	Regulation of transcription
228949_at	G protein coupled receptor 177	256	21	0,08	GPR177	Regulation of NF-kappaB cascade
224516_s_at	CXXC finger 5	525	99	0,19	CXXC5	Regulation of NF-kappaB cascade
204036_at	Endothelial differentiation, lysophosphatidic acid GPCR, 2	173	33	0,19	EDG2	Regulation of NF-kappaB cascade
200665_s_at	Secreted protein, acidic, cysteine-rich	163	21	0,13	SPARC	Tyrosine kinase signal transduction
58780_s_at	Hypothetical protein FLJ10357	599	118	0,20	FLJ10357	Rho protein signal transduction

Table 1. (Continued)

Probe set ID	Gene title	Classical	CD16- pos	Ratio	Gene symbol	Gene ontology biological process
205239_at	Amphiregulin	281	34	0,12	AREG	Cell–cell signaling
225175_s_at	Solute carrier family 44, member 2	123	617	5,00	SLC44A2	Transport
213395_at	Megalencephalic leukoencephalopathy with subcortical cysts 1	40	207	5,17	MLC1	Transport
214033_at	ATP-binding cassette, C (CFTR/MRP), member 6	182	18	0,10	ABCC6	Transport
223044_at	Solute carrier family 40, member 1	839	67	0,08	SLC40A1	Transport
217914_at	Two pore segment channel 1	776	111	0,14	TPCN1	Transport
219714_s_at	Ca-channel, voltage- dependent, alpha 2/delta 3 subunit	905	47	0,05	CACNA2D3	Transport
217897_at	FXYD domain containing ion transport regulator 6	339	60	0,18	FXYD6	Transport
226301_at	Chromosome 6 open reading frame 192	497	43	0,09	C6orf192	Transport
206130_s_at	Asialoglycoprotein receptor 2	1005	86	0,09	ASGR2	Endocytosis
244692_at	Cytochrome P450, family 4, subfamily F, polypeptide 22	27	316	11,53	CYP4F22	Electron transport
225987_at	STEAP family member 4	743	90	0,12	STEAP4	Electron transport
204961_s_at	Neutrophil cytosolic factor 1	1936	364	0,19	NCF1	Electron transport
212473_s_at	Microtubule associated monoxygenase	950	123	0,13	MICAL2	Electron transport
202436_s_at	Cytochrome P450, family 1, subfamily B, polypeptide 1	1751	199	0,11	CYP1B1	Electron transport
201627_s_at	Insulin-induced gene 1	163	1477	9,08	INSIG1	Lipid metabolic process
209555_s_at	CD36 molecule (thrombospondin receptor)	2856	388	0,14	CD36	Lipid metabolic process
213222_at	Phospholipase C, beta 1 (phosphoinositide-specific)	903	90	0,10	PLCB1	Lipid metabolic process
227038 ₋ at	Sphingomyelin synthase 2	469	90	0,19	SGMS2	Lipid metabolic process
213566_at	Ribonuclease, RNase A family, k6	4029	256	0,06	RNase6	RNA catabolic process
216667_at	Ribonuclease, RNase A family, 2	147	27	0,18	LOC643332	RNA catabolic process
206111_at	Ribonuclease, RNase A family, 2	2707	156	0,06	RNase2	RNA catabolic process
213397_x_at	Ribonuclease, RNase A family, 4	577	19	0,03	RNase4	RNA catabolic process
205141_at	Angiogenin, ribonuclease, RNase A family, 5	200	29	0,15	ANG	Angiogenesis
205767_at	Epiregulin	855	63	0,07	EREG	Angiogenesis
210512_s_at	Vascular endothelial growth factor A	664	33	0,05	VEGFA	Angiogenesis
206574_s_at	Protein tyrosine phosphatase type IVA, member 3	84	1037	12,41	PTP4A3	Protein amino acid dephosphorylation
220231_at	Chromosome 7 open reading frame 16	20	591	29,61	C7orf16	Protein amino acid phosphorylation
206028_s_at	c-mer proto-oncogene tyrosine kinase	103	529	5,13	MERTK	Protein amino acid phosphorylation
205559_s_at	Proprotein convertase subtilisin/kexin type 5	370	57	0,16	PCSK5	Signal peptide processing

Table 1. (Continued)

Table 1. (Continu						
Probe set ID	Gene title	Classical	CD16- pos	Ratio	Gene symbol	Gene ontology biological process
205174_s_at	Glutaminyl-peptide cyclotransferase	2112	153	0,07	QPCT	Protein modification process
209791_at	Peptidyl arginine deiminase, type II	791	110	0,14	PADI2	Protein modification process
203817_at	Guanylate cyclase 1, soluble, beta 3	18	315	17,93	GUCY1B3	cGMP biosynthetic process
220384_at	Thioredoxin domain containing 3	159	29	0,18	TXNDC3	GTP biosynthetic process
221942_s_at	Guanylate cyclase 1, soluble, alpha 3	30	221	7,47	GUCY1A3	cGMP biosynthetic process
221268_s_at	Sphingosine-1-phosphate phosphatase 1	79	744	9,40	SGPP1	Sphingolipid metabolic process
224918_x_at	Microsomal glutathione S-transferase 1	1695	145	0,09	MGST1	Glutathione metabolic process
235751_s_at	Vitelline membrane outer layer 1 homolog	17	277	16,60	VMO1	Vitelline membrane formation
200884_at	Creatine kinase, brain	30	375	12,68	CKB	Brain development
202967_at	Glutathione S-transferase A4	42	436	10,38	GSTA4	Response to stress
204647_at	Homer homolog 3	312	58	0,19	HOMER3	Protein targeting
242931_at	_	340	24	0,07	_	ATP-dependent proteolysis
221541_at	Cysteine-rich secretory protein LCCL domain containing 2	1040	64	0,06	CRISPLD2	Lung development
203184_at	Fibrillin 2	309	50	0,16	FBN2	Anatomical structure morphogenesis
209616_s_at	Carboxylesterase 1	826	58	0,07	CES1	Metabolic process
203305_at	Coagulation factor XIII, A1 polypeptide	1627	100	0,06	F13A1	Blood coagulation
206343_s_at	Neuregulin 1	814	17	0,02	NRG1	Nervous system development
201324_at	Epithelial membrane protein 1	242	30	0,12	EMP1	Cell death
211864_s_at	fer-1-like 3, myoferlin (C. elegans)	174	888	5,10	FER1L3	Muscle contraction
203060_s_at	3'-Phosphoadenosine 5'-phosphosulfate synthase 2	247	1438	5,82	PAPSS2	Sulfate assimilation
212224_at	Aldehyde dehydrogenase 1 family, member A1	1211	95	0,08	ALDH1A1	Metabolic process
202499_s_at	Solute carrier family 2, member 3	3328	506	0,15	SLC2A3	Carbohydrate transport
241525_at	Hypothetical protein LOC200772	26	1917	73,16	LOC200772	_
219955_at	LINE-1 type transposase domain containing 1	21	143	6,85	L1TD1	_
213069_at	HEG homolog 1 (zebrafish)	87	935	10,70	HEG1	_
227478 ₋ at	Hypothetical protein LOC284262	20	357	17,48	LOC284262	_
1553177_at	SH2 domain containing 1B	20	1281	64,03	SH2D1B	_
237753_at	Transcribed locus	19	163	8,55	_	_
236198_at	Transcribed locus	13	345	25,99	— EL 140405	_
229559_at	Hypothetical protein FLJ40125	46	497	10,71	FLJ40125	

Table 1. (Continued)

			CD16-		Gene	Gene ontology
Probe set ID	Gene title	Classical	pos	Ratio	symbol	biological process
229530_at	cDNA clone IMAGE:5302158	21	145	6,90	_	_
227235_at	cDNA clone IMAGE:5302158	17	254	15,33	_	_
227733_at	Transmembrane protein 63C	42	264	6,23	TMEM63C	_
205933_at	SET binding protein 1	35	440	12,52	SETBP1	_
236280_at	Transcribed locus	9	212	23,28	_	_
1562048 ₋ at	Hypothetical protein LOC152225	20	174	8,67	LOC152225	_
229629_at	Transcribed locus	13	262	19,56	_	_
1556656₋at	Full length insert cDNA clone YB31B05	37	187	5,08	_	_
219383_at	Hypothetical protein FLJ14213	47	435	9,33	FLJ14213	_
1556385 ₋ at	cDNA FLJ39926 fis, clone SPLEN2021157	99	687	6,93	_	_
221011_s_at	Limb bud and heart development homolog	29	213	7,25	LBH	_
226931 ₋ at	Transmembrane and tetratricopeptide repeat containing 1	38	228	6,00	TMTC1	_
238587 ₋ at	Ubiquitin associated and SH3 domain containing, B	94	541	5,73	UBASH3B	_
213915 ₋ at	Natural killer cell group 7 sequence	117	1152	9,89	NKG7	_
1555870_at	Ring finger protein 207	18	127	7,22	RNF207	_
223836_at	Fibroblast growth factor binding protein 2	20	408	20,87	FGFBP2	_
206548_at	Hypothetical protein FLJ23556	67	635	9,49	hCG_1776259	_
218865_at	MOCO sulphurase C-terminal domain containing 1	740	112	0,15	MOSC1	_
230778_at	Transcribed locus	208	34	0,16	_	_
227929 ₋ at	cDNA clone IMAGE:5277945	461	80	0,17	_	_
238365_s_at	Hypothetical LOC339541	444	42	0,09	MGC33556	_
242051_at	Transcribed locus	132	21	0,16	_	_
235568 ₋ at	Chromosome 19 open reading frame 59	2436	130	0,05	C19orf59	_
213839 ₋ at	KIAA0500 protein	284	54	0,19	KIAA0500	_
238778_at	MAGUK p55 subfamily member 7	594	62	0,10	MPP7	_
235109 ₋ at	cDNA FLJ40581 fis, clone THYMU2007729	179	35	0,19	_	_
226789_at	Embigin homolog (mouse) pseudogene	1999	235	0,12	LOC647121	_
213056_at	FERM domain containing 4B	167	29	0,18	FRMD4B	_
235735 ₋ at	Full length insert cDNA clone ZC64D04	897	162	0,18	_	_
1559776 ₋ at	cDNA FLJ36989 fis, clone BRACE2006753	629	83	0,13	_	_
244726 ₋ at	Transcribed locus	792	115	0,14	_	_
242494_at	Transcribed locus	382	74	0,19	_	_
1562289_at	cDNA DKFZp434N0220	441	57	0,13	_	_
229307_at	Ankyrin repeat domain 28	213	22	0,10	ANKRD28	_
228285_at	Tudor domain containing 9	274	53	0,19	TDRD9	_
208450₋at	Lectin, galactoside-binding, soluble, 2	2942	425	0,14	LGALS2	_
235490 ₋ at	Transmembrane protein 107	171	32	0,18	TMEM107	_
236571_at	Transcribed locus	544	78	0,14	_	_

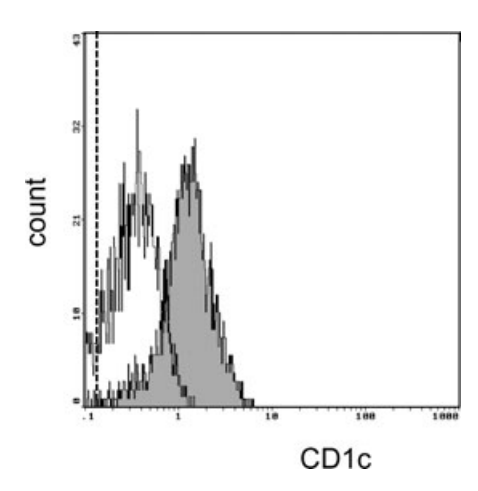


Figure 3. Purity of isolated CD1c⁺ blood dendritic cells (DCs). Mononuclear cells were isolated from peripheral blood by density gradient separation and DCs were purified by positive selection using MACS technology. Shown is a single-parameter FACS histogram of CD1c⁺ DCs (purity 96%). Data are representative of three independent experiments.

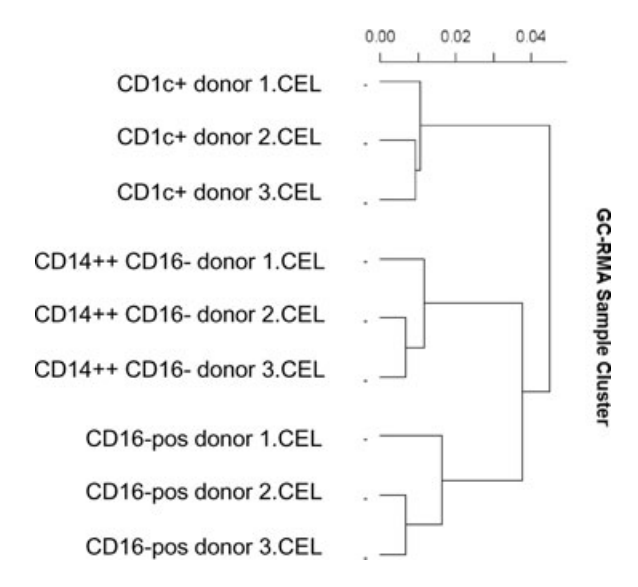
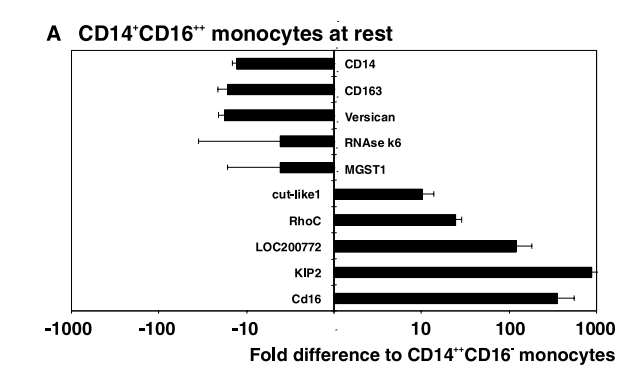


Figure 4. Hierarchical clustering of gene expression by monocyte subsets and CD1c⁺ blood DCs. Monocyte subsets and CD1c⁺ DCs from three different donors were purified, messenger RNA (mRNA) was isolated, labeled, and hybridized to Affymetrix U133 plus2 arrays. Expression data from CEL files were subjected to hierarchical clustering. Shown are from top to bottom results for CD1c⁺ blood DCs, classical CD14⁺⁺CD16⁻ monocytes and CD16-positive monocytes. Data are representative of three independent experiments.

are newly recruited cells, such that the contribution of the cells from the central pool to the RT-PCR signal is only one quarter. Analysis of the ten genes demonstrated the same pattern for the cells after exercise (Fig. 5B) compared with cells isolated at rest. These data suggest that CD16-positive monocytes arising from the central and the marginal pool are very similar in their gene expression. Therefore, cells isolated after exercise can be used for the study of gene expression in monocyte subsets.



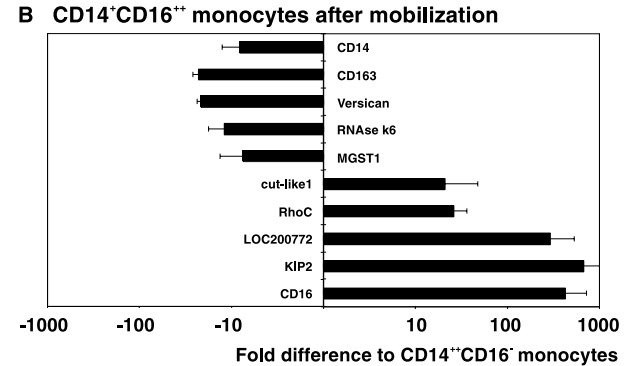


Figure 5. Gene expression for highly differential genes in monocytes before and after exercise. Monocyte subsets were isolated by MACS separation to >95% purity. Messenger RNA (mRNA) was purified and expression of CD14, CD16, versican, RNase k6, MGST1, cut-like 1, RhoC, LOC200772, kip 2, and CD163 was analyzed by RT-PCR. Expression in CD16-positive monocytes is expressed as fold difference compared with classical CD14++CD16- monocytes. Data are shown for (A) cells isolated from blood of healthy individuals at rest and (B) cells isolated from blood of healthy individuals after 1 min of exercise. For cut-like 1, LOC200772 and CD16 data from additional four donors were included. Data are shown as mean +SD of n=3-7 donors. Differences in gene expression between the CD16-positive and classical monocytes are significant at p<0.05 for all genes (Student's t-test).

Gene expression in macrophages derived from CD16-positive and CD14⁺⁺CD16⁻ classical monocytes

In order to address the question whether classical and CD16-positive monocytes are committed to become different types of macrophages we cultured monocytes in vitro for 7 days in the presence of M-CSF. A positive monocyte selection procedure, which involves binding of monoclonal antibodies such as anti-CD14 and anti-CD16 to the cells, may trigger the cells via these receptors and activate the monocytes when they are cultured subsequently at 37°C. In order to avoid artifacts brought about by such signals, we isolated monocyte subsets by no-touch procedures. Figure 6 demonstrates a high purity of more than 98% for both types of cells. Of note, these preparations still contain the PB lymphocytes, that is, the events in the lower left corner of the dot plots.

After culture in vitro for 7 days in the presence of M-CSF, both types of monocytes gave rise to monocyte-derived macrophages (MDMs) as indicated by an increase in forward and right angle light scatter (Fig. 7). These MDMs were then purified by positive selection using MACS technology and the purified cells were

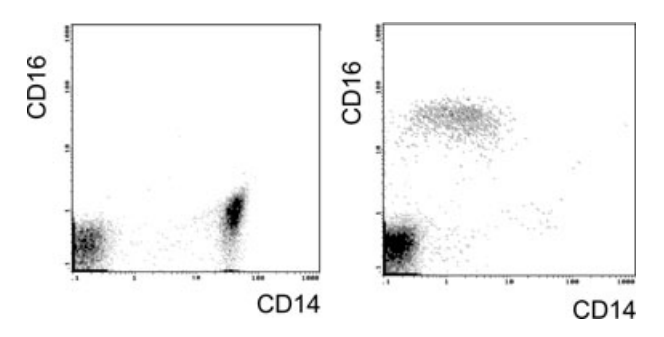


Figure 6. Purity of no-touch isolated blood monocyte subsets. Monocyte subsets were isolated by no-touch MACS technology to 99% as described in *Material and methods*. Lymphocyte population is shown in lower left corner of the plots. Data shown are representative of ten individual experiments.

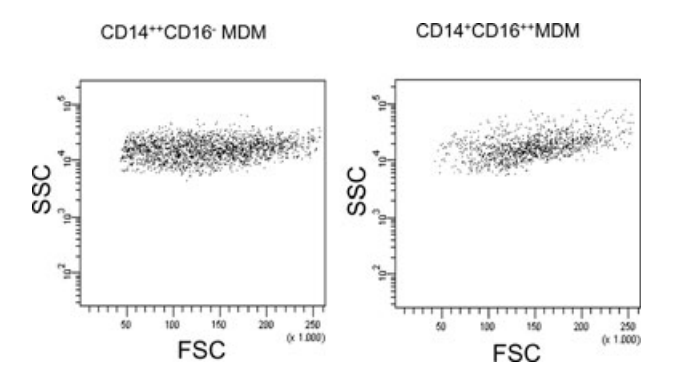


Figure 7. Both monocyte subsets give rise to MDMs. No-touch isolated classical and CD16-positive monocytes were culture in vitro for 7 days in the presence of M-CSF. Cells were then stained for CD64 and light scatter dot plots were generated. Data shown are representative of four independent experiments.

studied for gene expression by RT-PCR. Of the ten genes analyzed, three (CD14, CD163, and versican) maintained a differential expression between the MDMs derived from the classical and the CD16-positive monocytes. Figure 8 shows transcript levels nor-

malized to the expression level in classical monocytes and gives in each panel the classical monocytes on the left, the MDMs derived from the classical monocytes in the middle, and the MDMs derived from the CD16-positive monocytes on the right. When comparing the expression between the two types of MDM then we see a threefold, threefold, and 78-fold lower level in the progeny of the CD16-positive monocytes for CD14, CD163, and versican, respectively. These data indicate that the CD16-positive MDMs retain features of their monocyte progenitor cells. Also, when looking at phagocytosis of opsonized *E. coli* there is an average fourfold higher phagocytosis in the MDM derived from the CD16-positive monocytes (Fig. 9).

Gene expression in tissue macrophages

When analyzing various macrophage populations for the set of ten genes, we discovered that alveolar macrophages, small sputum macrophages, milk macrophages, and synovial fluid macrophages, all had a unique molecular fingerprint that was distinct from both the CD16-positive monocytes and classical monocytes.

The alveolar macrophages (Supporting Information Fig. 2) showed low CD14 and versican expression but high CD163 levels and very high induction of CD16, which in average was 1000-fold higher compared with the level seen in classical blood monocytes.

Sputum macrophages (Supporting Information Fig. 3) from patients with COPD were similar to alveolar macrophages with respect to CD14, versican, and CD163, but they showed lowered cut-like 1, LOC200772, and Kip2 levels genes that were increased in the alveolar macrophages.

Milk macrophages from nursing mothers (Supporting Information Fig. 4) gave a clearly different pattern with the CD14 level unchanged compared with the classical monocytes, that is, the absolute level of CD14 transcript is high. Versican decreased 1000-fold in these cells and CD16 transcripts decreased by factor 4.

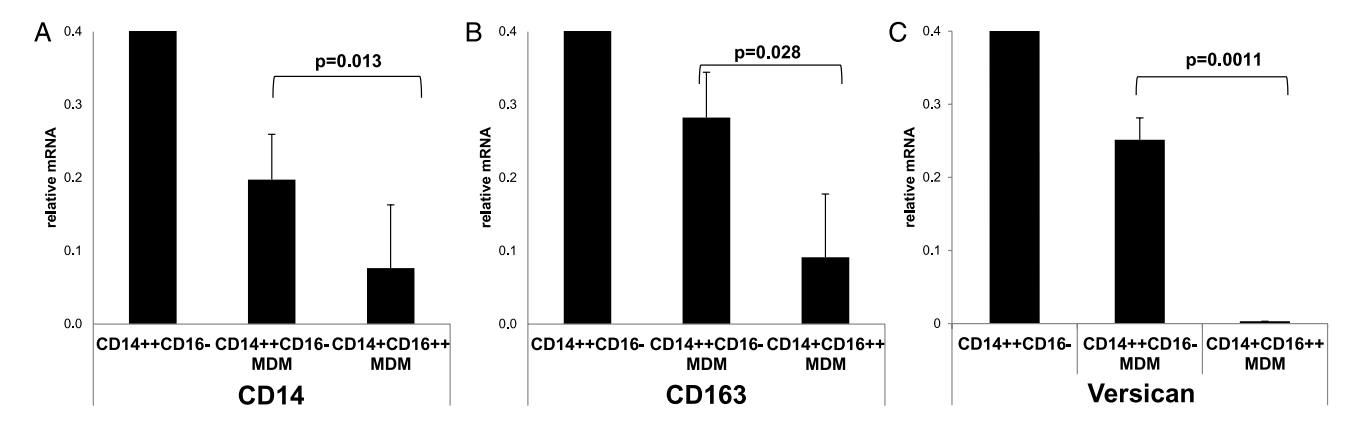


Figure 8. Gene Expression for CD14, CD163, and versican in macrophages derived from classical and nonclassical monocytes. Day 0 CD14⁺⁺CD16⁻ monocytes and day 7 MDMs derived from CD14⁺⁺CD16⁻ monocytes and from CD16-positive monocytes were isolated, messenger RNA (mRNA) was purified and reverse transcriptase polymerase chain reaction (RT-PCR) was performed for (A) CD14, (B) CD163, and (C) versican. The expression in CD14⁺⁺CD16⁻ monocytes is set at 1 for CD14 and CD163, and at 10 for versican. Expression in CD16-positive MDMs compared with CD14⁺⁺CD16⁻ MDMs was on average 2.58-fold lower for CD14, 3.1-fold lower for CD163, and 78-fold lower for versican. Data are shown as mean + SD of four donors. Statistical significance is determined by Student's t-test.

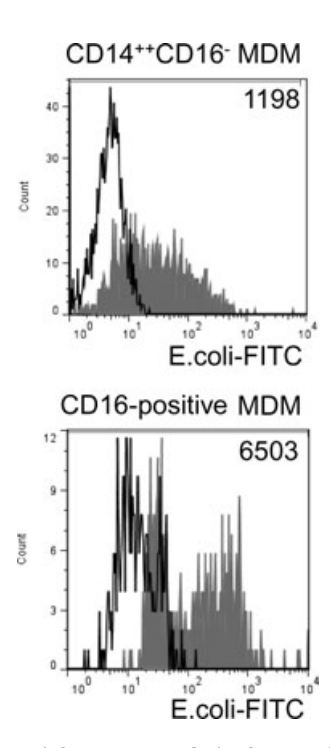


Figure 9. Phagocytosis by monocyte-derived macrophages (MDMs) derived from the two monocyte subsets. Monocyte subsets were isolated by no-touch procedures and cultured for 7 days in vitro. The macrophages were then incubated with opsonized FITC-labeled E. coli and phagocytosis was assessed by flow cytometry. Signal strength is given as specific mean fluorescence intensity and is shown at the upper right corner of the histogram. Data shown are representative of five independent experiments. Phagocytosis was on average 2739 \pm 1149 for the MDMs derived from classical monocytes and 13,951 \pm 10,620 for MDMs derived from CD16-positive monocytes (p < 0.05, Student's t-test).

Finally, synovial macrophages from patients with arthritis were studied (Supporting Information Fig. 5) and these cells showed the least change in the pattern of expression compared with the classical blood monocytes in that the transcript levels only changed by a factor of 5 or less for all genes but one. The only gene showing a more than tenfold induction was CD16 (25-fold).

The data demonstrate the pronounced heterogeneity of macrophages and they show that none of the populations tested is identical or similar to either the classical or the nonclassical blood monocytes.

Discussion

Our analysis of gene expression in the two monocyte subsets has revealed 187 genes that show a strongly differential expression. For these genes, the differences are at least fivefold and are consistently differentially expressed in the three individuals. For a selected set of genes, we could show that the difference at the transcript level also translates to a similar difference at the protein level. These data suggest that the differential gene expression in the two monocyte subsets will be biologically relevant for many of these genes. When looking at Gene Ontology, there is

a large group of differential genes that can be assigned to immune response and inflammation. Since monocytes are central cells in immune response and inflammation, any gene affecting the signal transduction, chemotaxis, and apoptosis of these cells will also directly impact on their contribution to immune response and inflammation. Therefore, a total of 89 genes can be assigned to these processes. In addition there are genes linked to lipid metabolism and angiogenesis, processes, in which monocytes and macrophages are known to play a prominent role. The present data suggest that the two types of monocytes may make a differential contribution to all these processes. Finally, there are genes without annotation but their strong differential expression indicates an important role for them, as well. Hence, a detailed analysis of every single of the 187 genes may demonstrate an important role in the function of the classical or the CD16-positive monocytes.

Ancuta et al. [14] have also analyzed the transcriptome of the monocyte subsets and they reported on 478 genes showing a ≥ twofold differential expression. In our analysis, we focused on genes with at least a fivefold difference in gene expression. Consistent with Ancuta et al., we find the same differential expression for IFIT, Siglec10, CDKN1c, CD14, and S100A12, genes that in the Ancuta study also show a high differential expression above or around fivefold. The transcriptome and proteome analysis of Zhao et al. [15] identified 521 genes with a differential expression of ≥ twofold with a large fraction of genes assigned to cell growth, proliferation and to cell death. In a further study [16], they then reported on a higher rate of apoptosis in the CD16-positive monocytes, which went along with a higher expression of pro-apoptotic genes including caspases and lower levels of anti-apototic genes such as SerpinB2 and TNFSF8. Our analysis, which focuses on at least fivefold differences, can confirm the differential expression of these genes (Table 1).

When the differential expression as seen in the array analysis was analyzed by RT-PCR and at the protein level by FACS, we found a consistent pattern with low expression for the IgA receptor and the CD163 haemoglobin receptor in the CD16-postive monocytes. The findings suggest that involvement of the nonclassical monocytes in IgA-mediated responses and clearance of haemoglobin may be much lower compared with the classical monocytes. Conversely, the higher expression of the IL-21 receptor and the IL-2 receptor beta chain (CD122) suggest that the nonclassical monocytes will show a stronger response to the respective ligands IL-21 and IL-2. CD79b is mainly expressed in B cells and is a crucial signal transduction molecule for the B-cell receptor. Nothing is known on the role of CD79b in monocytes/macrophages and a receptor, which associates with CD79b in these cells, still needs be identified. Our transcript and protein data for CD79b suggest that the CD16-positive monocytes may show a higher response upon engagement of a still elusive CD79b containing receptor complex.

To date, transcriptome analysis of monocyte subsets has been done at the constitutive level and this has shown dramatic differences that are consistent with a different functional repertoire of the two types of monocytes. Since much of the function of monocytes involves their gene expression after activation, it will be important to analyze the induced transcriptome of these cells in order to assess pro- and anti-inflammatory properties of the monocyte subsets.

Eur. J. Immunol. 2012. 42: 957-974

CD1c⁺ cells form a small group of blood DCs with high major histocompatibility complex (MHC) class II expression and high antigen-presenting cell (APC) activity [17, 18]. Our hierarchical clustering analysis reveals that the CD16-positive monocytes are more closely related to the classical CD14⁺⁺CD16⁻ monocytes than to the CD1c⁺ DCs. This is in line with the analysis presented by Robbins et al. [19], which employed data sets from Lindstedt et al. [20] and demonstrated that the CD16-positive monocytes cluster with myeloid cells, CD1c⁺ cells with blood DCs. Collectively, these data and our present analysis support the concept of separate lineages of monocytes and DCs in human blood with the CD16-positive cells being assigned to the monocyte lineage as proposed earlier [1].

In studies on the behavior of monocyte subsets after exercise we have noted a strong increase for the CD16-positive monocytes [13]. This has been seen by others and was linked to the action of catecholamines [13, 21]. Within minutes of exercise the numbers of CD16-positive monocytes will increase and they are back to normal after 20 min but can be induced again. These findings are consistent with the concept that the nonclassical monocytes preferentially reside in the marginal pool. The marginal pool is represented by cells, which within the vasculature localize to areas of low flow rate close to the endothelium [13]. This concept is supported by intravital microscopy data that show nonclassical monocytes in the mouse slowly moving on vascular endothelium [22] and this has been confirmed for human nonclassical monocytes injected into mice [23]. Our data in the present study show that the nonclassical monocytes in the central pool at rest and mobilized from the marginal pool after exercise show an identical gene expression pattern and hence can be considered to be identical cells.

The ten genes analyzed in this context were selected based on a strong differential expression and are of diverse function. The gene ontology for versican (extracellular matrix protein chondroitin sulfate proteoglycan 2) is cell adhesion, for RNase k6 it is RNA catabolic process for MGST1 (microsomal glutathione S-transferase 1), it is glutathione metabolic process, for cutlike 1 (cut-like homeobox1) it is regulation of transcription, for RhoC (Ras homolog gene family, member C) it is regulation of NF-κB cascade, for Kip2 (cyclin-dependent kinase inhibitor 1C) it is regulation of transcription, and LOC 200772 has not been assigned. The highly differential expression of these genes indicates that the monocyte subsets may be crucially involved in diverse processes unrelated to inflammation and immune defence. High expression of Kip2 in the CD16-positive monocytes for instance suggests that these cells may be refractory to proliferative signals.

When monocytes are isolated by positive selection with monoclonal antibodies against cell-surface molecules such as CD14 and CD16 followed by culture in vitro then we have to consider that CD14 and CD16 are receptors that can transduce signals, which can interfere with gene expression. In order to avoid this inter-

ference we have prepared no-touch isolated monocyte subsets and used these cells for subsequent culture and generation of macrophages. Highly purified monocytes can, however, undergo apoptosis and this is more pronounced in the nonclassical CD16-positive monocytes, most likely because these cells have higher levels of pro-apoptotic and lower levels of anti-apoptotic molecules [16]. This increased apoptosis can be avoided since we noted that survival is strongly improved when the cultures still contain lymphocytes, which may provide survival signals. The nature of cells and the signals involved are obscure at this point in time but this strategy allows for efficient generation of monocyte subset derived macrophages.

Our analysis of gene expression in the 7-day MDM has shown that the transcripts for CD14, CD163, and versican are lower in the progeny of nonclassical monocytes as compared with the progeny of the classical monocytes. Hence, for these genes the expression pattern is maintained, indicating that the macrophages generated from the different monocyte subsets are distinct. Also when it comes to phagocytosis we see a differential function with higher phagocytic activity in MDM derived from the nonclassical monocytes. For the nonclassical monocytes early reports have shown a higher phagocytosis of opsonized E. coli [5,24]. Hence this indicates that the higher phagocytic activity seen in the CD16-positive monocytes is maintained in the macrophage progeny. In more general terms, it indicates that a specific subset of monocyte is committed to become a specific type of macrophage. It will be important to analyze whether the intermediate CD14++CD16+ monocytes will also show evidence for a commitment to a distinct type of macrophage.

When looking at different macrophages obtained from human tissue, we found none that was identical to either the classical or the nonclassical monocytes. Still consistent with the developmental concepts in macrophage biology, these macrophages will derive from one of the blood monocyte subsets. Such a developmental relationship may be revealed by a more extensive gene analysis of human tissue macrophages. Furthermore, selective depletion of one subset followed by analysis of tissues can reveal a developmental relationship. There is, for instance, circumstantial evidence that Kupffer cells in the liver might derive from nonclassical monocytes in that depletion of the nonclassical monocytes in blood leads to depletion of Kupffer cells [25]. By contrast, macrophages in the lung are unaffected by this treatment. Consistent with these findings, our studies show a different pattern of gene expression for CD16-positive monocytes and alveolar and sputum macrophages (see Supporting Information Fig. 2 and 3). Human Kupffer cells were not available for the present study but analysis of gene expression in these cells may show a pattern similar to the CD16-positive monocytes and this would support a developmental relationship in man. Taken together, it may well be that tissue macrophages with a gene expression pattern similar to the CD16-positive monocytes can be identified by testing macrophages from additional types of tissues including the

In conclusion, we demonstrate herein a high number of genes, which show a pronounced differential expression between

monocyte subsets. Also, we show that the differential expression can be maintained in the macrophage progeny. This is consistent with the concept that the two different monocyte types are committed to become two different types of macrophages.

Materials and methods

Blood leukocytes

Heparinized venous blood at 10 U/mL was taken at rest or after mobilization by exercise [13] for 1 min at 200–400 W on a home trainer bike, in order to have higher recovery. Peripheral blood mononuclear cells (PBMCs) were isolated by density gradient separation and subpopulations (CD14⁺⁺CD16⁻, CD16-positive, and CD1c⁺CD19⁻) were purified by positive selection using MACS to give purities >90%. All samples from apparently healthy donors and patients were obtained after approval by the local Ethics Committee and after written informed consent.

CD14++CD16- monocytes touch separation

Isolation of CD14⁺⁺CD16⁻ monocytes was performed with one-third of PBMCs that were obtained by density gradient separation (LymphoPrep, density 1.077 g/ml, Nycomed, Oslo, Norway) from healthy volunteers. PBMCs were incubated with anti-CD16 microbeads (#130–045-701, Miltenyi, Bergisch-Gladbach, Germany) for 30 min on ice and cells were applied to an LD-column (#130–042-901, Miltenyi) positioned in a MidiMACS magnet (#130–042-302, Miltenyi). The effluent cells, which were depleted of CD16-positive monocytes, were then incubated with anti-CD14 microbeads (#130–050-201, Miltenyi) for 30 min on ice. These cells were then applied to a MS-column (#130–042-201, Miltenyi). After extensive washing, the column was removed from the magnet and the positive fraction was eluted. The resultant population was found to be >97% CD14-positive as determined by FACS analysis.

CD14⁺⁺CD16⁻ monocytes were then lysed at once in 2×10^4 cells/200 μ l TRI-reagent (#T9424, Sigma, Taufkirchen, Germany) for RT-PCR analysis. For array analysis, 3–4 \times 10⁶ cells were lysed in 200 μ l TRI-reagent.

CD16-positive monocytes touch separation

Isolation of CD16-positive monocytes was performed with the other two-thirds of PBMCs obtained after Ficoll separation. PBMCs were first incubated with anti-CD56 microbeads (#130–050-410, Miltenyi) for 30 min on ice and then applied to a LD-column as described above. The CD56 depleted effluent cells were then incubated with anti-CD16 micro beads again for 30 min on ice and CD16-positive monocytes were then separated positively over an MS-column. Purity was determined by staining with CD45-PC5/CD14-FITC/CD16-PE by FACS analysis.

Table 2. Monoclonal antibodies used for FACS analysis

Antigen	Dilution	Catalogue number	Supplier
CD14-PC5	1:20	#A07765	Beckman Coulter
CD16(3G8)-	1:20	#555406	Becton Dickinson
FITC			
CD79b-PE	1:20	#555679	Becton Dickinson
CD89-PE	1:20	#555686	Becton Dickinson
CD122-PE	1:40	#554525	Becton Dickinson
IL-21R-PE	1:20	#560264	Becton Dickinson
IgG1-PE	1:20	#555749	Becton Dickinson
CD163(Mac2-	1:20	#CD163-	iqproducts
158)-PE		158P	
IgG ₁ -PE	1:20	#IQP-191R	iqproducts

The CD16-positive monocytes were then lysed at once in 2×10^4 cells/200 μl TRI-reagent for RT-PCR analysis. For array analysis, 3–4 \times 10^6 cells were lysed in 200 μl TRI-reagent.

CD1c+CD19- blood DC touch separation

Isolation of blood DCs was performed by using the CD1c⁺ (BDCA-1) DC isolation kit from Miltenyi (#130–090-506) according to the manufacturer's instructions with PBMCs from 200 mL heparinized blood as initial volume. Purity over 90% (95.8 \pm 3%) was determined by FACS analysis and cells were lysed in aliquots of 5–10 \times 10⁵ in 200 μ l TRI-reagent to be used for cDNA expression arrays and in aliquots of 2 \times 10⁴ cells/200 μ l TRI-reagent for RT-PCR analysis.

Flow cytometry analysis of cell-surface markers on monocyte subsets

For three-color analysis of freshly isolated PBMCs, we used CD14-PC5/CD16(3G8)-FITC combined with a PE-conjugated monoclonal antibody (CD89, CD122, CD163, IL-121R) for surface staining or the respective isotype control IgG1-PE. For intracellular staining for CD79b expression, cells were permeabilized with Cytofix/Cytoperm (Becton Dickinson #554714, Heidelberg, Germany) for 30 min on ice and then stained for intracellular CD79b-PE. Monoclonal antibodies used for FACS staining are indicated in Table 2.

CD14++CD16- MDMs

CD14⁺⁺CD16⁻ MDMs were generated on day 0 from PBMCs that have been depleted from CD16-positive monocytes and were obtained by density gradient separation (LymphoPrep) from healthy volunteers. PBMCs were incubated with anti-CD16 microbeads (#130–045-701, Miltenyi) and anti-CD56 microbeads (#130–050-410, Miltenyi) for 30 min on ice and cells were applied to a LD-column (#130–042-901, Miltenyi) positioned in a Midi-

Eur. J. Immunol. 2012. 42: 957–974 Innate immunity 971

MACS magnet (#130-042-302, Miltenyi). The effluent PBMCs, which were depleted of CD16-positive monocytes and found to be more than 95% enriched with CD14++CD16- cells in the monocyte gate as determined by FACS analysis, were then seeded in 24-well ultra low attachment plates (#3473, Costar, Germany) at $1 \times 10^6 / mL$ per well in culture medium +10% fetal calf serum (FCS) and supplemented with 100 ng M-CSF/ml. Culture medium consisted of Roswell Park Memorial Institute (RPMI) 1640 (#1415, Biochrom, Berlin, Germany) supplemented with L-glutamine 2 mM (#25030-024, Invitrogen, Karlsruhe, Germany), penicillin 200 U/ml, streptomycin 200 µg/mL (#15140-114, Invitrogen), nonessential amino acids 1-2× (#11140-35, Invitrogen), and 10 mL for 1 l OPI media supplement (#O-5003, Sigma) containing oxalacetic acid, sodium pyruvate, and insulin. To avoid any inadvertent LPS contamination, we used a culture medium that was filtered through a Gambro ultrafilter U 2000 (#N50316001, Gambro, Martinsried, Germany). All cells with contaminating lymphocytes were harvested on day 7 and MDM further enriched positively with anti-CD64-FITC (#IM1604U, Beckman Coulter, Krefeld, Germany) and anti-FITC microbeads (#120-000-293, Miltenyi) as secondary antibody on a LS-column (#130-042-401, Miltenyi). Purity was determined by staining with CD45-PC5/CD14-FITC/CD16-PE by FACS analysis to be greater than 92%. Resulting CD14++CD16- MDM were then lysed at once in 2 \times 10⁴ cells/200 μ l TRI-reagent for RT-PCR analysis.

CD16-positive MDMs

CD16-positive MDMs were generated on day 0 from PBMCs that were depleted of CD14++CD16- monocytes and were obtained by density gradient separation (LymphoPrep) from healthy volunteers. PBMCs were incubated with anti-CD15 microbeads (#120-000-262, Miltenyi), anti-CD56 microbeads (#130-050-410, Miltenyi), 1% anti-CD14 microbeads (#130-050-201, Miltenyi), anti-CCR2 (#MAB150, R&D Systems, Wiesbaden, Germany), and anti-CD64 (#MCA756G, AbD Serotec, Düsseldorf, Germany) for 30 min on ice. After a washing step in D-PBS and incubation for 30 min on ice with goat anti-mouse microbeads (#120-000-288, Miltenyi) as secondary antibody, cells were applied to a LD-column (#130-042-901, Miltenyi) positioned in a MidiMACS magnet (#130-042-302, Miltenyi). The effluent PBMCs, which were depleted of CD14++CD16- monocytes and found to be more than 90% enriched with CD16-positive cells in the monocyte gate as determined by FACS analysis, were then seeded in 24-well ultra low attachment plates (#3473) at 1×10^6 /mL per well in culture medium as noted above and supplemented with 100 ng M-CSF/ml. All cells with contaminating lymphocytes were harvested on day 7 and MDM further enriched positively with anti-CD64-FITC (#IM1604U) and anti-FITC microbeads (#120-000-293, Miltenyi) as secondary antibody on a LS-column (#130-042-401, Miltenyi) as described for the CD14++CD16- MDM. Purity was determined by staining with CD45-PC5/CD14-FITC/CD16-PE

by FACS analysis to be greater than 92%. Resulting CD16-positive MDM were then lysed at once in 2 \times 10 4 cells/200 μl TRI-reagent for RT-PCR analysis.

Alveolar macrophages

Bronchoalveolar lavage was performed as described previously [26] for routine diagnostic purposes in patients with sarcoidosis or other inflammatory lung diseases. The percentage of CD14+ macrophages was additionally determined by FACS analysis. The mean percentage of macrophages in the samples used was 60 \pm 4.4%. Alveolar macrophages, and at the same time, isolated CD14++CD16- blood monocytes by MACS touch separation were lysed at once after isolation at 2 \times 10^4/200 μ l TRI-reagent.

Sputum macrophages

Sputum induction and processing

Sputum induction and processing were carried out as previously described [27,28] with some modifications. Briefly, for induction of induced sputum chronic obstructive pulmonary disease (COPD) patients were asked to inhale sterile saline solutions of 0.9% up to 3%. The aerosol was generated by using a multisonic nebulizer at maximum output for 5 min. Donors were then asked to blow their nose and rinse their mouths with water. The participants were encouraged to cough vigorously into a Petri dish. In total, saline inhalation was performed for no longer than 10 min, and sputum was processed immediately on ice. Sputum (1 volume) was then admixed with four times the volume of Sputolysin, reconstituted according to the manufacturer's instructions (#560000, Calbiochem, San Diego, CA). The sputum/Sputolysin mixture was placed in a waterbath at 37°C for up to 20 min. An equal volume of PBS (pH 7.4) was added subsequently. The resultant cell suspension was then filtered through 100 and 40 µm Falcon cells sieves (#352360 and #352340, BD Sciences, Mannheim, Germany) to remove aggregates. Cells were centrifuged at 800g for 10 min at 4°C. The cell pellet was assessed for cell viability using the Trypan blue exclusion method. Cells were further resuspended in PBS (2% FCS) for flow cytometry staining of an aliquot before the RosetteSep procedure.

RosetteSep isolation of sputum macrophages

In order to obtain highly purified sputum macrophages the cell suspension was further processed using the RosetteSep method as previously described [29]. For this 3 mL cell suspension, mononuclear cell-depleted erythrocytes (30 μ l; obtained following centrifugation over LymphoPrep gradient) and 50 μ l monocyte enrichment cocktail (RosetteSep monocytes enrichment reagent, #15068, Stem Cell Technologies via Cell Systems, St. Katharinen, Germany) were added and incubated at room temperature

for 20 min. Cells were then diluted 1:1 with tissue-culture grade PBS, layered over an equal volume of LymphoPrep density gradient medium and centrifuged at 800g for 30 min to generate a mononuclear layer, which was aspirated, washed, and resuspended in LPS-free PBS/2% FCS solution. Cells were counted and viability was determined using Trypan blue. Sputum macrophages purified to more than 90% were then analyzed by flow cytometry or further used for RT-PCR. For analysis of array genes, only samples from COPD patients with more than 75% small macrophages were processed.

Breast milk macrophages

From three nursing mothers, we obtained 20–50 mL breast milk. Milk was immediately processed as described previously [26]. Aliquots with 2 \times 10⁴ breast milk macrophages (BMMs) were lysed at once in 200 μl TRI-reagent. Purity of the obtained BMMs was analyzed in flow cytometry by staining with CD14-FITC (My4, Beckman Coulter) and CD16-PE (Leu-11c, BD Biosciences, Heidelberg, Germany) and was 96.5 \pm 0.8% in the donors used. At the same time, CD14⁺⁺CD16⁻ blood monocytes were isolated by MACS separation from the same donors.

Synovial macrophages

Synovial fluid was obtained during routine diagnostic purposes from four patients with different forms of arthritis after informed consent. The synovial fluid was admixed with equal volumes of RPMI 1640 medium without supplements, layered over LymphoPrep solution, and further processed as for PBMC isolation. Obtained leukocytes were then incubated with anti-CD14-MB (Miltenyi) for 30 min at 4°C , and synovial macrophages were positively separated over a Miltenyi LD-column. Obtained synovial macrophages had mean purity of 92.7 \pm 5.4% determined by FACS analysis. At the same time, CD14++CD16- blood monocytes were positively isolated by MACS-separation from the same donors.

Phagocytosis assay

MDMs, derived from classical and CD16-positive monocytes, were harvested on day 7. Cells were washed once with culture medium and counted. For phagocytosis $2–5\,\times\,10^6$ cells/100 μl medium were incubated without or with the same amount of antibody-opsonized <code>Escherichia coli-Alexa Fluor 488</code> (Molecular Probes <code>#E-13231</code> and <code>#E-2870</code>; Life Technologies, Darmstadt, Germany) for 30 min at 37°C. Cells were then counterstained with CD163-PE (Trillium <code>#CD163-158P</code>, IQ Products, Groningen, The Netherlands) for 20 min on ice and washed with PBS/2% FCS. Cells were then resuspended in 750 μl PBS/2% FCS, and for quenching of fluorescence of extracellular bacteria, the same volume of 0.4% Trypan blue was added. Cells were then analyzed on a LSR II flow cy-

tometer with gating on CD163-positive macrophages. Results are given as delta mean fluorescence intensity between untreated and *E. coli* treated Trypan blue quenched samples.

Quantitative RT-PCR by LightCycler analysis

Quantitative PCR for all selected array mRNAs was performed as previously described [26, 30]. In brief, lysates containing 2×10^4 cells in 200 µl TRI-reagent were thawed and spiked with 15 µg transfer RNA from Brewer's yeast (Roche Diagnostics, Mannheim, Germany) as a carrier. Total RNA was isolated according to the manufacturer's instructions by phenol/chloroform extraction followed by a precipitation step in isopropanol and a final washing step in 75% ethanol. For further processing and storage, RNA was resolved in 20 μ l H₂O/DEPC. Equal amounts of each sample were reverse transcribed with oligo(dT) as a primer. Quantitative PCR was performed using the LightCycler system (Roche Diagnostics) with 3 μ l of cDNA per capillary in the SYBR Green format using the LightCycler-FastStart DNA Master SYBR Green I Kit from Roche (#2, 239, 264). As an external control, the housekeeping gene α-Enolase was amplified under the same conditions (annealing at 60°C). For a better comparison, data were corrected to the α -Enolase amount and set as 1 for all genes in the $CD14^{++}CD16^{-}$ monocytes as reference cells. Primer pairs are indicated in Table 3.

Transcriptional profiling

Monocyte subsets and the CD1c⁺ blood DCs, purified from three volunteers, were lysed in 200 μl TRI-reagent for further isolation of the RNA to be used for cDNA expression arrays. In brief, RNA was purified according to the manufacturers' instructions for Light-Cycler analysis, but by using 10- μg linear acrylamide (#AM9520 Ambion, Austin, TX) instead of transfer RNA for the precipitation step. Purified RNA was resolved in 20 μl H₂O/DEPC for further analysis.

Microarray sample labeling and hybridization

Total RNA (1 μ g) was amplified and labeled using the Affymetrix One-Cycle Target Labeling Kit (Freiburg, Germany) according to the manufacturer's recommendations. As newly transcribed RNA mainly consists of mRNA, it was amplified and labeled according to the manufacturer's protocol for mRNA. The amplified and fragmented biotinylated complementary RNA (cRNA; 15 μ g) was hybridized to Affymetrix U133 plus2.0 arrays using standard procedures.

Microarray data processing and statistical analysis

The experimental setup contains a total of nine arrays, made up of three groups, and each group of three biological replicates.

Table 3. Primer pairs used for quantitative RT-PCR

	Forward primer (5' \rightarrow 3')	Reverse primer (5' \rightarrow 3')
CD14	CCC TAG CGC TCC GAG ATG	CCA AGG CAG TTT GAG TCC AT
CD163	GCC AGA CGC TGG GGC CAT A	ATC ATC TGC ATT CAG GCA AG
Versican	ACA AGC ATC CTG TCT CAC G	TGA AAC CAT CTT TGC AGT GG
RNase k6	AAA ATA CCT TTC TGC ATG A	CGG GAA CAA GAA AATCAA CAA
MGST1	ATT TCT TGG AAT TGG CCT CCT	AAT GGG TTT ACC CCA GTT CA
LOC200772	CAG TGT TGG GGA GGT AAC GC	AAG CCC ACT TCT CTG ACT GC
Kip2	GGC CTC TGA TCT CCG ATT TC	GGG ACC AGT GTA CCT TCT CG
RhoC	GAG CCC GTT CGG TCT GAG	GCA GGA GGG AAC TGA AAA TG
cut-like 1	CCC GGC CAG GCT AAG CCG	TCT CTC TCT TGG GGT GCA GT
CD16	GGT CAT TTG TCT TGA GGG TC	CAC CTG AGG TGT CAC AGC T
α-Enolase	GTTAGCAAG AAACTGAACGTCACA	TGA AGG ACT TGT ACA GGT CAG
CD79b	ACG AGG GCC TGG ACA TTG AC	ACC TCA TAG CAC CCC CAG A
CD89	TGT ATG GCA AAC CCT TCC TC	GAG GCT TCC TTG TTC AGT GC
CD122	GAC AAG CGT TGA GCC ACT AA	AAT GTA ACC CTC CCA AGA AGT G
IL-21R	TTT CTC CTG GCT GAG AGC AT	ACA AGC AGG AGG AGA AGC AG

Arrays were assessed for quality and robust multi-array average (RMA)-normalized. Quality assessment consisted of RNA degradation plots, Affymetrix quality control metrics, sample crosscorrelation, and probe-level visualizations. Normalization incorporated (separately for each RNA-type data set) background correction, quantile normalization, and probe-level summation by RMA. The data were analyzed for differential gene expression using an empirical Bayes moderated t-test [31], implemented in the Bioconductor package Linear Models for Microarray Data LIMMA. The results were sorted by the adjusted p-value and exported in tab-delimited format. Microarray data have been submitted to the GEO database (http://www.ncbi.nlm.nih.gov/geo/) and have the accession number GSE18565 for monocyte subsets and GSE34515 for CD1c DCs.

Statistics

In addition to the bioinformatic statistics described above, Student's t-test was employed for all other comparisons.

Acknowledgments: We acknowledge the expert technical assistance of Gisela Jaskiola, Jörg Mages, Gudrun Kaßner, and Silvia Weidner. This work was supported by DFG Grant Zi 288 to LZH and DFG Transregio 22 to Thorsten Buch and Reinhard Hoffmann.

Conflict of interest: None of the authors state any financial or commercial conflict of interest.

References

- 1 Ziegler-Heitbrock, L., Ancuta, P., Crowe, S., Dalod, M., Grau, V., Hart, D. N., Leenen, P. J., Liu, Y. J. et al., Nomenclature of monocytes and dendritic cells in blood. Blood 2010. 116: e74-e80.
- 2 Fingerle-Rowson, G., Angstwurm, M., Andreesen, R. and Ziegler-Heitbrock, H. W., Selective depletion of CD14+ CD16-positive monocytes by glucocorticoid therapy. Clin. Exp. Immunol. 1998. 112: 501-506.
- 3 Dayyani, F., Belge, K. U., Frankenberger, M., Mack, M., Berki, T. and Ziegler-Heitbrock, L., Mechanism of glucocorticoid-induced depletion of human CD14+CD16-positive monocytes. J. Leukoc. Biol. 2003. 74:
- 4 Ziegler-Heitbrock, L., The CD14+ CD16-positive blood monocytes: their role in infection and inflammation. J. Leukoc. Biol. 2007. 81: 584-592.
- 5 Nockher, W. A. and Scherberich, J. E., Expanded CD14+ CD16-positive monocyte subpopulation in patients with acute and chronic infections undergoing hemodialysis. Infect. Immun. 1998. 66: 2782-2790.
- 6 Fingerle-Rowson, G., Auers, J., Kreuzer, E., Fraunberger, P., Blumenstein, M. and Ziegler-Heitbrock, L. H., Expansion of CD14+CD16-positive monocytes in critically ill cardiac surgery patients. Inflammation 1998. 22: 367-
- 7 Weiner, L. M., Li, W., Holmes, M., Catalano, R. B., Dovnarsky, M., Padavic, K. and Alpaugh, R. K., Phase I trial of recombinant macrophage colony-stimulating factor and recombinant gamma-interferon: toxicity, monocytosis, and clinical effects. Cancer Res. 1994. 54: 4084-4090.
- 8 Wong, K. L., Tai, J. J., Wong, W. C., Han, H., Sem, X., Yeap, W. H., Kourilsky, P. et al., Gene expression profiling reveals the defining features of the classical, intermediate, and nonclassical human monocyte subsets. Blood 2011. 118: e16-e31.
- 9 Ingersoll, M. A., Spanbroek, R., Lottaz, C., Gautier, E. L., Frankenberger, M., Hoffmann, R., Lang, R. et al., Comparison of gene expression profiles between human and mouse monocyte subsets. Blood 2010. 115: e10-
- 10 Ashburner, M., Ball, C. A., Blake, J. A., Botstein, D., Butler, H., Cherry, J. M., Davis, A. P. et al., Gene ontology: tool for the unification of biology. The Gene Ontology Consortium. Nat. Genet. 2000. 25: 25–29.

- 11 Randolph, G. J., Sanchez-Schmitz, G., Liebman, R. M. and Schakel, K., The CD16(†) (FcgammaRIII(†)) subset of human monocytes preferentially becomes migratory dendritic cells in a model tissue setting. *J. Exp. Med.* 2002. 196: 517–527.
- 12 Ziegler-Heitbrock, H. W., Fingerle, G., Strobel, M., Schraut, W., Stelter, F., Schutt, C., Passlick, B. et al., The novel subset of CD14⁺/CD16-positive blood monocytes exhibits features of tissue macrophages. Eur. J. Immunol. 1993 23: 2053–2058
- 13 Steppich, B., Dayyani, F., Gruber, R., Lorenz, R., Mack, M. and Ziegler-Heitbrock, H. W., Selective mobilization of CD14(+)CD16(+) monocytes by exercise. Am. J. Physiol. Cell Physiol. 2000. 279: C578–C586.
- 14 Ancuta, P., Liu, K. Y., Misra, V., Wacleche, V. S., Gosselin, A., Zhou, X. and Gabuzda, D., Transcriptional profiling reveals developmental relationship and distinct biological functions of CD16-positive and CD16-monocyte subsets. BMC Genomics 2009. 10: 403.
- 15 Zhao, C., Zhang, H., Wong, W. C., Sem, X., Han, H., Ong, S. M., Tan, Y. C. et al., Identification of novel functional differences in monocyte subsets using proteomic and transcriptomic methods. J. Proteome Res. 2009. 8: 4028–4038
- 16 Zhao, C., Tan, Y. C., Wong, W. C., Sem, X., Zhang, H., Han, H., Ong, S. M. et al., The CD14(+/low)CD16(+) monocyte subset is more susceptible to spontaneous and oxidant-induced apoptosis than the CD14(+)CD16(-) subset. Cell Death Dis. 2010. 1: e95.
- 17 Thomas, R. and Lipsky, P. E., Human peripheral blood dendritic cell subsets. Isolation and characterization of precursor and mature antigenpresenting cells. J. Immunol. 1994. 153: 4016–4028.
- 18 Dzionek, A., Fuchs, A., Schmidt, P., Cremer, S., Zysk, M., Miltenyi, S., Buck, D. W. et al., BDCA-2, BDCA-3, and BDCA-4: three markers for distinct subsets of dendritic cells in human peripheral blood. *J. Immunol.* 2000. 165: 6037–6046.
- 19 Robbins, S. H., Walzer, T., Dembele, D., Thibault, C., Defays, A., Bessou, G., Xu, H. et al., Novel insights into the relationships between dendritic cell subsets in human and mouse revealed by genome-wide expression profiling. Genome Biol. 2008. 9: R17.
- 20 Lindstedt, M., Lundberg, K. and Borrebaeck, C. A., Gene family clustering identifies functionally associated subsets of human in vivo blood and tonsillar dendritic cells. J. Immunol. 2005. 175: 4839–4846.
- 21 Kittner, J. M., Jacobs, R., Pawlak, C. R., Heijnen, C. J., Schedlowski, M. and Schmidt, R. E., Adrenaline-induced immunological changes are altered in patients with rheumatoid arthritis. Rheumatology (Oxford) 2002. 41: 1031– 1039.
- 22 Auffray, C., Fogg, D., Garfa, M., Elain, G., Join-Lambert, O., Kayal, S., Sarnacki, S. et al., Monitoring of blood vessels and tissues by a population of monocytes with patrolling behavior. Science 2007. 317: 666–670.
- 23 Cros, J., Cagnard, N., Woollard, K., Patey, N., Zhang, S. Y., Senechal, B., Puel, A. et al., Human CD14dim monocytes patrol and sense nucleic acids and viruses via TLR7 and TLR8 receptors. *Immunity* 2010. 33: 375–386.
- 24 Mosig, S., Rennert, K., Krause, S., Kzhyshkowska, J., Neunubel, K., Heller, R. and Funke, H., Different functions of monocyte subsets in familial hypercholesterolemia: potential function of CD14+ CD16positive monocytes in detoxification of oxidized LDL. FASEB J. 2009. 23: 866–874.

- 25 MacDonald, K. P., Palmer, J. S., Cronau, S., Seppanen, E., Olver, S., Raffelt, N. C., Kuns, R. et al., An antibody against the colony-stimulating factor 1 receptor depletes the resident subset of monocytes and tissue- and tumor-associated macrophages but does not inhibit inflammation. Blood 2010. 116: 3955–3963.
- 26 Frankenberger, M., Schwaeble, W. and Ziegler-Heitbrock, L., Expression of M-Ficolin in human monocytes and macrophages. Mol. Immunol. 2008. 45: 1424–1430.
- 27 Frankenberger, M., Menzel, M., Betz, R., Kassner, G., Weber, N., Kohlhaufl, M., Haussinger, K. et al., Characterization of a population of small macrophages in induced sputum of patients with chronic obstructive pulmonary disease and healthy volunteers. Clin. Exp. Immunol. 2004. 138: 507–516.
- 28 Wright, A. K., Rao, S., Range, S., Eder, C., Hofer, T. P., Frankenberger, M., Kobzik, L. et al., Pivotal Advance: Expansion of small sputum macrophages in CF: failure to express MARCO and mannose receptors. J. Leukoc. Biol. 2009. 86: 479–489.
- 29 Frankenberger, M., Eder, C., Hofer, T. P., Heimbeck, I., Skokann, K., Kassner, G., Weber, N. et al., Chemokine expression by small sputum macrophages in COPD. Mol. Med. 2011. 17:762–770.
- 30 Frankenberger, M., Haussinger, K. and Ziegler-Heitbrock, L., Liposomal methylprednisolone differentially regulates the expression of TNF and IL-10 in human alveolar macrophages. Int. Immunopharmacol. 2005. 5: 289– 299.
- 31 Smyth, G. K., Linear models and empirical bayes methods for assessing differential expression in microarray experiments. Stat. Appl. Genet. Mol. Biol. 2004. 3: Article3.

Abbreviations: COPD: chronic obstructive pulmonary disease · Kip2: cyclindependent kinase inhibitor 1C · MGST1: microsomal glutathione Stransferase 1 · MDM: monocyte derived macrophage · RhoC: Ras homolog gene family, member C · RMA: robust multi-array average

Full correspondence: Prof. Loems Ziegler-Heitbrock, Helmholtz Center Munich, EvA Study Center, Robert-Koch-Allee 29, 82131 Gauting, Germany

Fax: +49-89-3187-19-1889

E-mail: ziegler-heitbrock@helmholtz-muenchen.de

Current addresses: Ayman Marei, Micobiology & Immunology Department, Immunology Research Unit, Zagazig University, Egypt.

Farshid Dayyani, Genitourinary Medical Oncology, MD Anderson Cancer Center, The University of Texas, Houston, TX, USA.

Asaad Aldraihim, National Centre of Biotechnology, King Abdulaziz City for Science and Technology (KACST), Riyadh, Saudi Arabia.

Roland Lang, Institute of Clinical Microbiology, Immunology and Hygiene, University Hospital Erlangen, Germany.

Received: 30/6/2011 Revised: 31/6/2011 Accepted: 22/12/2011

Accepted article online: 1/4/2012